Nanoscale Res Lett (2010) 5:1102–1106
DOI 10.1007/s11671-010-9608-z

NANO EXPRESS

Surfactant-Assisted in situ Chemical Etching for the General Synthesis of ZnO Nanotubes Array

Hongqiang Wang · Ming Li · Lichao Jia · Liang Li · Guozhong Wang · Yunxia Zhang · Guanghai Li

Received: 22 March 2010 / Accepted: 9 April 2010 / Published online: 24 April 2010

Abstract In this paper, a general low-cost and substrate-independent chemical etching strategy is demonstrated for the synthesis of ZnO nanotubes array. During the chemical etching, the nanotubes array inherits many features from the preformed nanorods array, such as the diameter, size distribution, and alignment. The preferential etching along *c* axis and the surfactant protection to the lateral surfaces are considered responsible for the formation of ZnO nanotubes. This surfactant-assisted chemical etching strategy is highly expected to advance the research in the ZnO nanotube-based technology.

Keywords ZnO · Nanotubes array · Chemical etching · Surfactant · Substrate independent

Introduction

One-dimensional (1D) nanostructures are of particularly interest due to their unique properties different from that of bulk and nanoparticles [1–5]. It is well known that the hollow nanostructures have more prominent advantages (such as the enhanced confinement effect and larger area–volume ratios) over the other 1D nanostructures, such as nanowires and nanorods, and thus are promising candidates in catalysts, gas sensors, phosphors, and solar cells [6–9]. Zinc oxide (ZnO), with a direct band gap of 3.37 eV and a high exciton binding energy of 60 meV at room temperature, is an important technological semiconductor due to its distinguished optical, electrical, and piezoelectrical properties [10, 11]. Various kinds of 1D ZnO nanostructures array, such as nanorods, nanobelts, nanoneedles, and nanotips, have recently been synthesized by a good number of techniques [10, 11]. In contrast, only limited studies have been reported on the fabrication of ZnO nanotubes array, which is probably because the tubular form is generally available in layered materials such as carbon nanotubes. Current synthesis of ZnO nanotubes array is mainly based either on the chemical vapor deposition or the electrochemical approach [12–17], which generally requires economically prohibitive temperatures and complex processes, and is unfavorable for mass production. Additionally, despite the good controllability realized by the electrochemical method, the growth of ZnO nanotubes array can only be achieved on the conductive substrates, which greatly confines the wide applications of the resulted nanotubes in many other fields (such as gas sensing, which generally utilize nonconductive quartz substrates). Exploring strategy for a general low-cost and substrate-independent fabrication of ZnO nanotubes array is thus highly desirable.

Recently, a controllable synthesis of 1D novel nanostructures with different morphologies has been realized in our group by using various chemical etching methods [18–20], in which the preferential etching along *c* axis was found to be an important etching behavior for ZnO polar crystal. In this paper, by using the surfactant as the

Electronic supplementary material The online version of this article (doi:10.1007/s11671-010-9608-z) contains supplementary material, which is available to authorized users.

H. Wang (✉) · M. Li · L. Jia · L. Li · G. Wang · Y. Zhang · G. Li (✉)
Key Laboratory of Materials Physics, Anhui Key Laboratory of Nanomaterials and Nanotechnology, Institute of Solid State Physics, Chinese Academy of Sciences, 230031 Hefei, People's Republic of China
e-mail: hqwang@issp.ac.cn

G. Li
e-mail: ghli@issp.ac.cn

protection layer to the nonpolar surfaces of ZnO nanorod, we demonstrate a surfactant-assisted chemical etching approach to synthesize the ZnO nanotubes array. This chemical etching strategy is substrate independent and facile in manipulation, thus provides an avenue of a general and low-cost fabrication of the ZnO nanotubes array, which is highly expected to advance the ZnO nanotube-based technology.

Experimental

Typically, ZnO nanocrystals were spin coated onto silicon wafer to form a seed layer according to the literature [21], and hydrothermal growth was carried out by suspending the silicon wafer upside down in an autoclave filled with an aqueous solution of 6 ml ammonia (25 wt%) and 80 ml zinc chloride solution (0.1 M) at 95°C for 70 min (growth step). After growth, the wafer was thoroughly rinsed with de-ionized water and suspended once again into a 90 ml solution containing ammonia (0.5 wt%) and cetyltrimethyl ammonium bromide (CTAB; 0.5 wt%) at room temperature for 3.5 h (etching step) and then washed with de-ionized water again. The as-synthesized samples were characterized by X-ray diffraction (XRD, Philips X'pert PRO), field emission scanning electron microscopy (FE-SEM, Sirion 200), and transmission electron microscopy (TEM, JEOL 2010, 200 kV). A He–Cd laser system with the excitation wavelength of 325 nm was used to investigate the photoluminescence properties of the final products.

Results and Discussion

Figure 1a shows the FESEM image of the ZnO nanorods obtained in the growth step, in which the nanorods with an average size of about 200 nm and flat termination can be clearly seen (inset in Fig. 1a). After the surfactant-assisted in situ chemical etching (etching step), tubular structures were formed, as shown in Fig. 1c. One can see that the nanotubes array inherits many features from the nanorods array, such as the diameter, size distribution, and alignment. The corresponding XRD pattern shown in Fig. 1b and d all indicate that the ZnO nanorods and nanotubes have a wurtzite (hexagonal) ZnO structure. It is interesting to note that the intensity of the (0002) diffraction peak at $2\theta = 34.4°$ for the nanotubes array decreases substantially when compared with that for the nanorods array.

The typical TEM image of a single ZnO nanotube is shown in Fig. 2a, in which an obvious contrast between the tube wall and the inner part can be clearly observed, providing a direct evidence of the tubular structure. The selected area electron diffraction pattern shown in Fig. 2b demonstrates the single crystalline feature of the ZnO nanotube. Figure 2c shows the corresponding HRTEM image of the ZnO nanotube, in which the measured

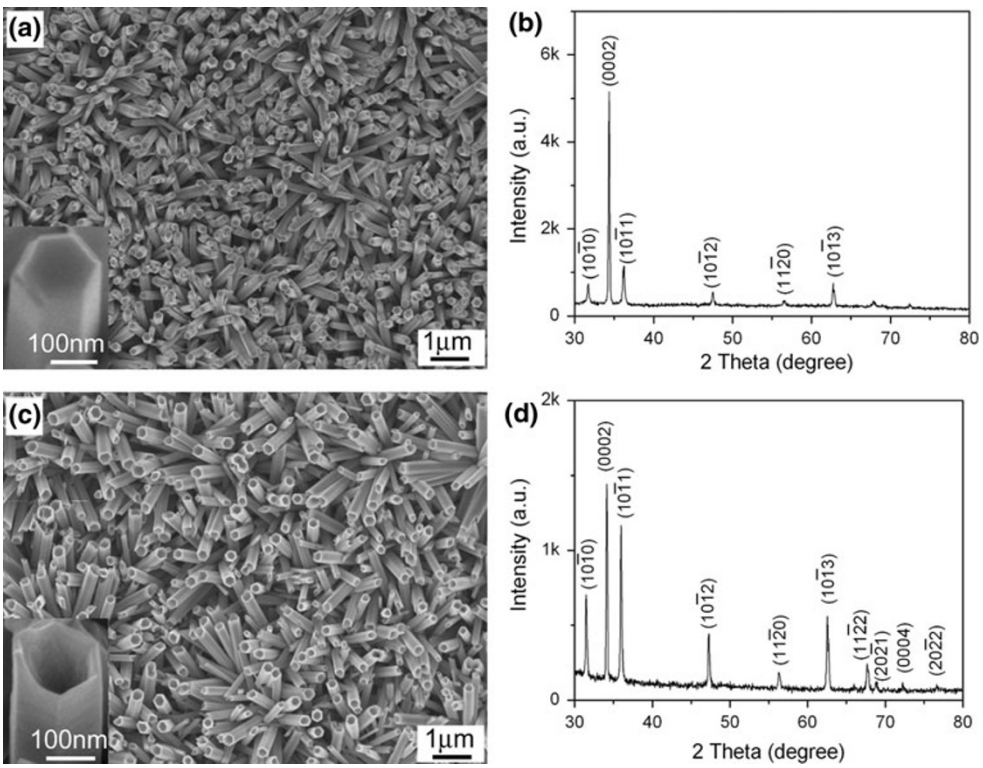

Fig. 1 **a** SEM image and **b** XRD pattern of the ZnO nanorods array, inset in **a** is the high-magnification image of a ZnO nanorod; **c** SEM image and **d** XRD pattern of the ZnO nanotubes array, inset in **c** is the high-magnification image of a ZnO nanotube

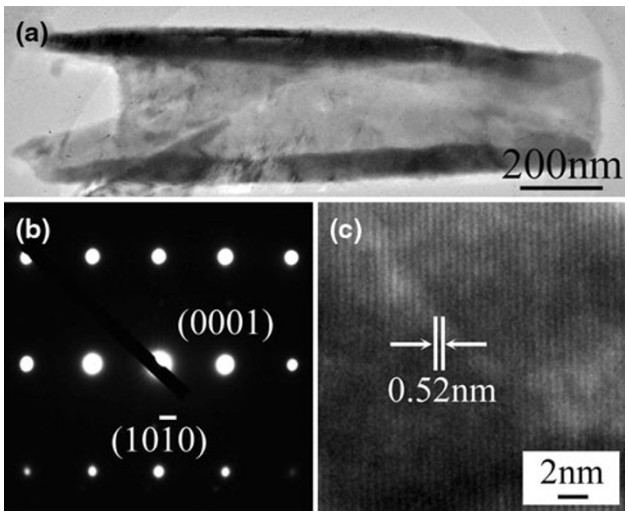

Fig. 2 **a** TEM, **b** SAED, and **c** HRTEM images of a single ZnO nanotube obtained by surfactant-assisted in situ chemical etching strategy

interplane spacing (0.52 nm) matches well with the literature reported value of the (0001) plane in wurtzite ZnO, indicating that the nanotube grows along the (0001) direction.

To investigate the formation mechanism of the ZnO nanotubes array, experiments with different etching time were performed (keeping other experimental conditions unchanged). Figure 3 shows the FESEM image of the product after etching for 0, 0.5, 1, and 1.5 h, respectively. Before etching, as shown in Fig. 3a, each nanorod obtained in the growth step has a flat termination. After etching for 0.5 h, the central part of the flat termination was firstly etched away, as shown in Fig. 3b, forming a very shallow pit at the top end of the nanorod. As the etching continued, a deeper and wider pit was formed on the top of the ZnO nanorod (see Fig. 3c, d). Prolonging the etching time leads to the further deepening of the hollow part and the final formation of the tubular structure.

It was found that the using of the surfactant in the etching step is much critical for the formation of the tubular nanostructure. If CTAB is not used in the etching process, the ZnO nanorods will become shorter and shorter (always with shallow pits at the top end) and finally be etched into the broken pieces (Figure S1). Too much CTAB used in the etching step (over 2 wt%) will lead to the formation of a thin surfactant coat on the surface of ZnO nanorods array, and thus block the subsequent etching (Figure S2). In addition, the amount of ammonia used in the etching step is also important for the controllable fabrication of ZnO nanotubes array. In the etching step, too much (larger than 5 wt%) or too little (lower than 0.1 wt%) amount of ammonia will result in the fast dissolution of ZnO nanorods array or no effect on the morphology change of ZnO nanorods.

From the above discussion, one can see that the formation of the nanotubes array undergoes two steps, the growth and the surfactant-assisted etching of the ZnO nanorods array, which can be described by reaction (1). In the growth step, the precursor $Zn(NH_3)_4^{2+}$ reacts with OH^- to form ZnO, and the equilibrium in Eq. (1) moves to the right side, corresponding to the deposition of ZnO, which only happens at temperatures higher than 75°C. In the

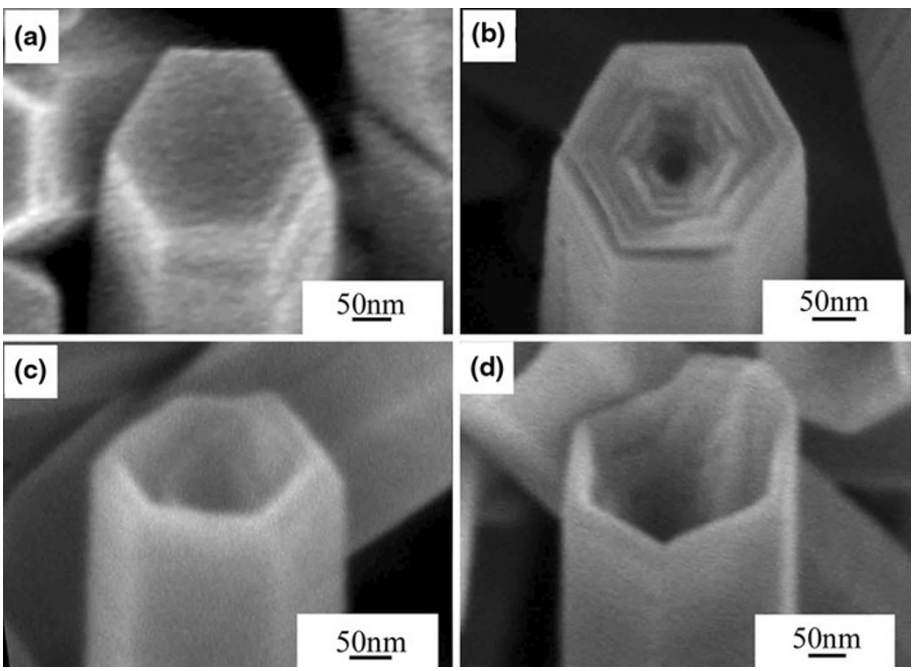

Fig. 3 FESEM images of products obtained by the surfactant-assisted in situ chemical etching strategy using different etching time **a** 0 h, **b** 0.5 h, **c** 1 h, and **d** 1.5 h

etching step, because the reaction proceeds at room temperature, the equilibrium in Eq. (1) will shift to the left side, leading to the etching of ZnO [22].

$$Zn(NH_3)_4^{2+} + OH^- \rightleftharpoons ZnO + NH_3 + H_2O \quad (1)$$

As is well known, ZnO is a polar crystal, and *c* axis is the most active direction both for the crystal growth and for the etching. In addition, the etching for ZnO also demonstrates a curvature dependency [18]. NH_3 is a polar molecule, and there exists a lone pair of electrons in its electronic structure. Because ZnO surface is also negatively/positively charged, the polar molecules of NH_3 can be easily attached on. For the location with higher curvature, the area density of the surface charges is higher, therefore, the electrostatic adhesion of NH_3 on ZnO nanorod is stronger, leading to a faster etching rate in this area. For free etching (without the surfactant), as shown in Fig. 4a, the etching is preferentially along the *c* axis, and that is why a shallow pit firstly forms. Then, the preferential etching location is replaced by the edge area of the shallow pit due to the much higher curvature. After the etching away of the top area, etching along *c* axis becomes dominant. Therefore, the alternatively dominant etchings result in the shorter and shorter of the ZnO nanorod, and always with a shallow pit on the top end, as shown in Fig. 4a. It has been reported that some surfactants such as SDS and CTAB can be used as effective agents to control the diameter of ZnO nanorod because these molecules can be firmly bonded by the lateral surfaces [23, 24]. Therefore, we speculate that the preferential etching along *c* axis and the surfactant protection to the lateral surfaces are responsible for the formation of ZnO nanotubes, as schematically illustrated in Fig. 4b, in which the CTAB protection to lateral surface of the top end of ZnO nanorod prevents the further etching of shallow pit edge, thus provides an obstacle for the curvature-dependent etching at the top end of ZnO nanorod and facilitates the etching along *c* axis.

It is easily understood that another possibility in producing ZnO nanotubes array is to combine the growth and etching into one step, i.e. after the growth of the ZnO nanorods array, directly decreasing the temperature from 95 to below 75°C, without taking out the silicon wafer. However, it was found that the resulted product was nanorods array with the similar feature obtained in the above-mentioned growth step, which might be due to the low NH_3 concentration dissolved in the reaction solution.

The room temperature photoluminescence spectra of the ZnO nanotubes array shown in Fig. 5 (the red curve) exhibits the typical near-band-gap ultraviolet emission centered at 396 nm and a broad visible emission band, which is usually attributed to deep-level emission caused by defects of oxygen vacancies. It is observable that the etching of the nanorod array in diluted etching solution does not influence the band edge emission intensity but causes a 8-nm red shift from 387 to 395 nm. Such a red shift might be related to the lattice strain due to the heterogeneous etching at the surface of the nanorod [7, 25], which can be evidenced by the enhanced intensity of the defects related emission (see Fig. 5). In addition, the changing of the dielectric environment and consequent renormalization of ZnO band structure induced by screening of the surfactant molecules might also contribute to the red shift.

The surfactant-assisted in situ chemical etching strategy presented in this study is general, and other substrates (polymers, ITO glasses, ceramic tubes/plates, etc.) also can be used to fabricate the ZnO nanotubes array via the same chemical etching process, which allows for the applications

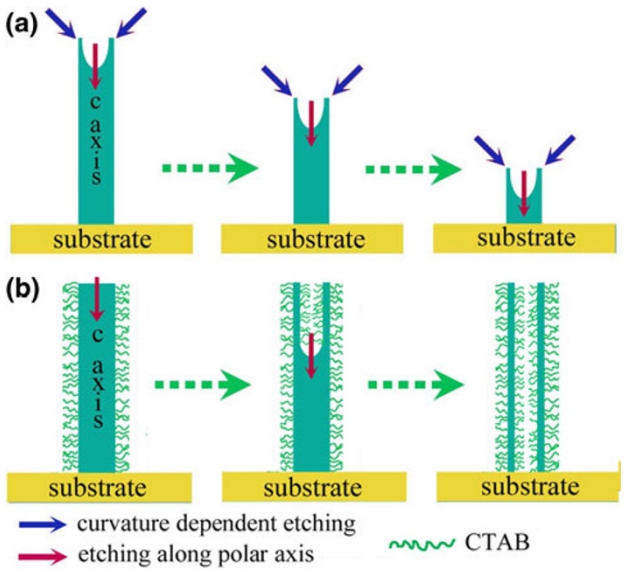

Fig. 4 Schematic illustration of the chemical etching of ZnO nanorods array: **a** free etching; **b** using the surfactant of CTAB

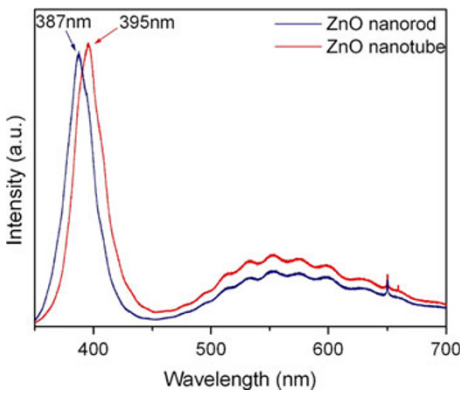

Fig. 5 PL spectra of the ZnO nanorods array (*blue curve*) and nanotubes array (*red curve*)

of ZnO nanotubes array in many fields, such as electronics, photocatalysis, and gas sensing. Additionally, the easy mediation in the diameter of the preformed nanorod array [23, 24] in the growth step makes it possible to produce the ZnO nanotubes with different diameters.

Conclusions

In summary, a general low-cost and substrate-independent synthesis of ZnO nanotubes array via a surfactant-assisted chemical etching strategy is demonstrated. The as-obtained ZnO nanotubes array shows an intensive ultraviolet photoluminescence emission, indicating the nanotubes array is promising for application in future nanoscale optoelectronic devices. The preferential etching along *c* axis and the surfactant protection to the lateral surfaces are considered responsible for the formation of ZnO nanotubes. This surfactant-assisted chemical etching strategy is highly expected to advance the research in the ZnO nanotube-based technology.

Acknowledgments This work was supported by the National Natural Science Foundation of China (No: 10904145 and No: 10704074), and the Anhui Natural Science Foundation (No: 090414188).

References

1. X.S. Fang, Y. Bando, M.Y. Liao, U.K. Gautam, C.Y. Zhi, B. Dierre, B.D. Liu, T.Y. Zhai, T. Sekiguchi, Y. Koide, D. Golberg, Adv. Mater. **21**, 2034 (2009)
2. H.B. Zeng, X.J. Xu, Y. Bando, U.K. Gautam, T.Y. Zhai, X.S. Fang, B.D. Liu, D. Golberg, Adv. Funct. Mater. **19**, 3165 (2009)
3. B.Q. Cao, X.M. Teng, S.H. Heo, Y. Li, S.O. Cho, G.H. Li, W.P. Cai, J. Phys. Chem. C **111**, 2470 (2007)
4. J.Q. Hu, Y. Bando, D. Golberg, J. Mater. Chem. **19**, 330 (2009)
5. H.Q. Wang, G.Z. Wang, L.C. Jia, C.J. Tang, G.H. Li, J. Phys. Chem. C **111**, 14307 (2007)
6. J.P. Liu, Y.Y. Li, H.J. Fan, Z.H. Zhu, J. Jiang, R.M. Ding, Y.Y. Hu, X.T. Huang, Chem. Mater. **22**, 212 (2010)
7. H.Q. Wang, G.Z. Wang, L.C. Jia, C.J. Tang, G.H. Li, J. Phys. D Appl. Phys. **40**, 6549 (2007)
8. S. Banerjee, S.K. Mohapatra, M. Misra, Chem. Commun. 7137 (2009)
9. T. Kawano, H.C. Chiamori, M. Suter, Q. Zhou, B.D. Sosnowchik, L.W. Lin, Nano Lett. **7**, 3686 (2007)
10. D.P. Norton, Y.W. Heo, M.P. Ivill, K. Ip, S.J. Pearton, M.F. Chisholm, T. Steiner, Mater. Today **7**, 34 (2004)
11. Z.L. Wang, J. Phys. Condens. Matter **16**, R829 (2004)
12. L. Li, S.S. Pan, X.C. Dou, Y.G. Zhu, X.H. Huang, Y.W. Yang, G.H. Li, L.D. Zhang, J. Phys. Chem. C **111**, 7288 (2007)
13. Y. Xi, J. Song, S. Xu, R. Yang, Z. Gao, C. Hu, Z.L. Wang, J. Mater. Chem. **19**, 9260 (2009)
14. C.C. Wu, D.S. Wuu, P.R. Lin, T.N. Chen, R.H. Horng, Crys. Growth Des. **9**, 4555 (2009)
15. H. Yu, Z. Zhang, M. Han, X. Hao, F. Zhu, J. Am. Chem. Soc. **127**, 2378 (2005)
16. G.W. She, X.H. Zhang, W.S. Shi, X. Fan, J.C. Chang, C.S. Lee, S.T. Lee, C.H. Liu, Appl. Phys. Lett. **92**, 053111 (2008)
17. L. Xu, Q. Liao, J. Zhang, X. Ai, D. Xu, J. Phys. Chem. C **111**, 4549 (2007)
18. H.Q. Wang, G.H. Li, L.C. Jia, G.Z. Wang, L. Li, Appl. Phys. Lett. **93**, 153110 (2008)
19. H.Q. Wang, G.H. Li, L.C. Jia, G.Z. Wang, C.J. Tang, J. Phys. Chem. C **112**, 11738 (2008)
20. H.Q. Wang, G.H. Li, L.C. Jia, L. Li, G.Z. Wang, Chem. Commun. 3786 (2009)
21. C. Pacholski, A. Kornowski, H. Weller, Angew. Chem. Int. Ed. **41**, 1188 (2002)
22. A. Wei, X.W. Sun, C.X. Xu, Z.L. Dong, Y. Yang, S.T. Tan, W. Huang, Nanotechnology **17**, 1740 (2006)
23. E. De la Rosa, S. Sepulveda-Guzman, B. Reeja-Jayan, A. Torres, P. Salas, N. Elizondo, M.J. Yacaman, J. Phys. Chem. C **111**, 8489 (2007)
24. A. Dev, S.K. Panda, S. Kar, S. Chakrabarti, S. Chaudhuri, J. Phys. Chem. B **110**, 14266 (2006)
25. C.L. Hsu, S.J. Chang, Y.R. Lin, S.Y. Tsai, I.C. Chen, Chem. Commun. 3571 (2005)